Journal of
Biomedical Nanotechnology
Vol. 3, 120–130, 2007

Transport of Biologically Active Molecules to Intracellular Environments Utilizing a Lyzosomally Cleavable Random Block Copolymer of Polyethylenimine

A. Braden[1,*], M. Roner[2], J. Ganter[3], and K. Nelson[4]

[1] *University of North Texas Health Science Center, Department of Molecular Biology and Immunology, Fort Worth, TX, USA*
[2] *University of Texas at Arlington, Department of Biology, Arlington, TX, USA*
[3] *Departamento de Bioquímica, Universidade Federal do Paraná, C.P. 19046, 81531-990 Curitiba (Pr), Brazil*
[4] *TissueGen Inc., Dallas, TX, USA*

The use of cationic polymers for the delivery of DNA to mammalian cells has generated significant interest due to the intrinsic properties associated with these delivery vector systems. One particular system utilizing polyethylenimine (PEI) has been rigorously investigated. A major drawback associated with PEI is the cytotoxicity of the vector/delivery system. In an effort to combat this adverse side effect we have synthesized a novel random block copolymer based upon low molecular weight PEI. Here we report the grafting of EGS (ethylene glycol bis(succinimidyl succinate)), to a low molecular weight PEI. Upon cellular transfection, introduction of two carboxylester bonds from the bioconjugation process are cleavable within the lytic pathways of the cell. We confirm the successful grafting of this agent through FITR and C-13 NMR. Molecular weight determination of the grafted copolymer was performed through HPLC-SEC and light scattering experiments. This polymer retains the ability to deliver GFP encoding plasmid DNA to 3T3 fibroblasts. Transfection levels were found to be approximately 90%. Transfection of T7 RNA dependent DNA polymerase was also performed utilizing our copolymer. We find successful activation of a virally introduced RNA transcript.

Keywords: Polyethylenimine, Polymeric Delivery, Vaccinia Virus, Cationic.

1. INTRODUCTION

Cationic polymers provide unique delivery systems for the formation of gene therapy devices. One such polymer, polyethylenimine (PEI) has been the subject of a large number of investigations. PEI can be synthesized through a cationic ring opening polymerization of aziridines or oxazolines, leading to a branched or linear form respectively.[1–4] An extremely advantageous property of this class of non-viral gene delivery systems is the inherent charge interactions between DNA and the polymeric backbone. The association between the polymer and the DNA is so avid that in our, and others, experiments, a protective barrier from mechanical, chemical, and naturally occurring degradation (DNAse and serum) is established.[3,4]

It has been proposed that the uptake of PEI into the cell is through endocytosis.[3–6] Based on this assumption, it follows that the transport of a DNA/PEI complex across the cellular membrane must then endure localization to intracellular lytic pathways. Other groups have fluorescently labeled the DNA/PEI complex and subsequently observed fluorescence within the cell nucleus.[3,4,6,7] This data, along with the assumption of transfection via an endocytic pathway implies that PEI complexed DNA avoided degradation within the acidic environment of the lysosome, and therefore that the PEI must have served as a "proton sponge" protecting the DNA during the delivery process.[8] Despite all the positive benefits associated with the formulation of potential gene therapy systems using PEI, several issues remain unclear.

Following modification of PEI, encapsulation properties should remain the same. Transfection efficiency appears to depend to a large extent upon the surface charge of the polycation[1,19] and the molecular weight of the DNA/PEI complex.[19] Targeting of PEI with folate or PEG-folate-PEI has shown the ability to transfect cells over expressing

*Author to whom correspondence should be addressed.

 1550-7033/2007/3/120/011 doi:10.1166/jbn.2007.013

folate receptor.[8] It has been found that while specific targeting is possible, transfection efficiencies have not been dramatically increased. Similar results have been seen using transferrin modified PEI.[9, 10] The speculation has therefore become that a reduction in the surface charge of the PEI is more significant when attempting to increase the transfection efficiency.[1] The synthetic pathways utilized in our group, by virtue of ablation of primary amine moieties within the PEI backbone, accomplish this reduction in charge density. To control the ultimate molecular weight, reaction conditions can be tuned such that only a fraction of the primary amines are ablated.

Another alternative that is beginning to be investigated is the use of enhanced biocompatible cationic polymers. Synthesis of a PEG-PEI random block copolymer showed mixed transfection results when compared to unmodified PEI.[11–14] Enhanced transfection was noticed with pegylated PEI however the size of the molecule was an important factor.[11] The grafting of cholesterol to the surface of low molecular weight PEI had little effect.[15] The incorporation of galactose with poly(ethylene glycol) PEI showed only a two fold increase in transfection efficiency.[16] Thus far, improvements in the biocompatibility of PEI have not yet led to greater transcription of delivered plasmid DNA.

In an effort to overcome some of the potential obstacles associated with transfection using non-viral systems, optimization of a polyethylenimine based system was undertaken. In order to enhance delivery of bioactive agents, native PEI was grafted to ethylene glycol bis(succinimidyl succinate) (EGS), a cleavable cross-linking reagent within lytic intracellular compartments. This process should allow for two key factors to occur. First, biocompatibility of native PEI should be greatly improved due to intracellular cleavage of the grafted PEI analog, allowing for the reduction of an apparent large molecular weight polymer into a lower "monomeric" molecular weight polymer. This reduction should correspond with a decrease in cellular cytotoxicity, hence an improvement in biocompatibility. Second, there should also be enhanced transfection of the bioactive agents due to the increase in polymeric molecular weight associated with the grafting process and the rapid reduction of the polymer within the cell.

2. METHODS

2.1. Chemicals

PEI of molecular weight 1.2 kD and 10 kD was purchased from Polysciences Inc. (Warrington, PA). Plasmid DNA containing the T7 bacterial promoter element upstream of the green fluorescent protein (GFP) coding sequence (pQBI T7-GFP) was purchased from Quantum Biotechnologies (Montreal, Canada). Vaccinia virus encoding the T7 promoter element for the β-galactosidase gene (Vv-T7-LZ) was obtained courtesy of Dr. Bernard Moss (NIH). TRITC and ethidium bromide were purchased from Sigma-Aldrich Chemicals (St. Louis, MO) T7 RNA dependent DNA polymerase was purchased from Stratagene (La Jolla, CA). EGS (ethylene glycol bis(succinimidyl succinate)) and Dithiobis(succinimidyl propionate), [DSP] were obtained from Pierce Biotechnology (Rockford, IL).

2.2. Synthesis of PEI Grafted EGS (EPI)

The synthetic pathway for the generation of EPI is as follows. 2.4 g of PEI (2.0 mM) was added to 1.5 ml of distilled deionized water. 11.4 mg of EGS (0.025 mM) was solubilized in 10% DMSO and distilled deionized water. This corresponds to an ablation of 5 percent of the reactive primary amines present on the PEI monomer (primary amine starting concentration is 0.5 mM) under 100% reaction conditions. Solubilized EGS and PEI were combined and the pH adjusted to 7.2 by the drop wise addition of hydrochloric acid. The reaction was allowed to progress for 6 h until completion at room temperature.

2.3. Characterization of EPI

The structure of the grafted copolymer was characterized through several methods. FTIR spectroscopy was performed using a Bruker Vector-22 spectrophotometer. Calcium fluoride windows were purchased from Pike Technologies. HPLC analysis was performed on an Akta Purifier (Pharmacia Biotech) using a Jordi Gel Polar Pac Wax Mixed Bed column (Jordi Associates). The solvent used was 95%/5% distilled deionized water/acetic acid at a flow rate of 1.0 ml/min. Detection of the analyte was performed using a Shodex RI-71 refractive index detector and a UV detector. Further structural characterization was performed using C-13 NMR spectroscopy (300 MHz, Varian Instruments). NMR samples were prepared by the addition of 50 mg of reaction product to distilled deionized water. The addition of 1% w/v of trifluoroacetic acid was performed to set a reference peak.

Light scattering data was acquired using a DAWN EOS light scattering detector (Wyatt Technology Corp., Santa Barbara, CA). The laser wavelength was 690 nm. Determination of the molecular weight is performed through extrapolation of the scattering angle data to a calculated zero scattering angle, and the concentrations analyzed to a zero concentration value. The point of intersection from the extrapolated concentration and scattered light lines gives the estimated molecular weight. This information is represented in a Zimm plot. For Zimm plot generation under static conditions five concentrations of EPI were prepared by serial dilution and were transferred to Wheaton scintillation vials for analysis. The concentrations analyzed were, 5.35 mg/ml, 2.675 mg/ml, 1.34 mg/ml, 0.664 mg/ml, and 0.334 mg/ml. All samples were filtered using a 0.1 μm syringe filter.

2.4. Agarose Gel Electrophoresis

To ensure that EPI retained the capability for DNA binding/complex formation, an electrophoretic mobility shift assay (EMSA) was performed. Complexes of DNA and polymer were formed at various N/P ratios. The ratios studied were 0.75, 0.56, 0.44, and 0.36. The DNA/EPI complexes were incubated at room temperature for 10 minutes and subsequently run on a 0.7% agarose gel. Retardation of the complexes was visualized with Ethidium bromide.

2.5. pH Buffering Capacity of EPI

To determine the ability of the synthetic product to serve as an effective pH buffering agent, a titration reaction was established. 250 mg of PEI at 1.2 kD and 10 kD as well as EPI were brought to a pH of 10 using 1 N Sodium hydroxide. The addition of 20 μl of 1 N hydrochloric acid was then carried out and the pH monitored. 1 N Hydrochloric acid was added in a repeated administration of 20 μl aliquots and the pH monitored until a minimum pH of 4.0 was seen.

2.6. Self Capture of T7-GFP Using Cationic Polymer Supports

The capture of T7-GFP plasmid DNA with either native PEI or the grafted PEI analog EPI was carried out by mixing 4 μg of plasmid DNA with 500 ng of the polymer in an aqueous solution. Incubation was carried out at room temperature for a minimum of 15 minutes. Immediately after capture the cationic polymer/plasmid DNA complexes were exposed to cells.

2.7. Coupling of T7 DNA Polymerase to Cationic Polymer Supports

Dithiobis(succinimidyl propionate), [DSP] was solubilized in a 30% DMSO/70% distilled deionized water solution. Dialyzed T7 polymerase was mixed with the cationic polymer (PEI or EPI) to which coupling was desired. The introduction of 0.025 mM DSP into the polymer and polymerase solution initiated the reaction. These reaction conditions should ablate 5% of the primary amines on the PEI or PEI analog, EPI. The reaction was carried out at pH 7.3 in 4 °C for 6 h. The reaction products were stored at 4 °C overnight, and warmed to 37 °C prior to exposure to cells.

2.8. Infection and Transfection Protocols

Murine 3T3 cells were employed for the transfection assays. Cells were seeded at 25,000 cells per cell culture slide well. The cells were incubated overnight at 37 °C. The following day viral infection was initiated. For plasmid DNA transfection using a cationic polymer the cells were initially infected with vaccinia virus that contained the T7 polymerase (Vv-T7). The infections with Vv-T7 were carried out at an M.O.I. of 2.5 for 45 minutes at 37 °C. Following incubation with the virus, viral containing media was aspirated off and the cationic polymer containing T7-GFP plasmid DNA was exposed to the cells (10 kD PEI, EPI). Following 1.5 hours of incubation at 37 °C cells were examined using laser confocal microscopy.

For transfection of T7 DNA polymerase/PEI complexes a similar process was followed. In this series of transfections, vaccinia virus encoding β-galactosidase RNA with the T7 promoter element upstream (Vv-T7-LZ) was used to infect the cells. Following 45 minutes of exposure to virus at an M.O.I. of 5 the virus containing media was aspirated off. Cationic polymer to which T7 polymerase had been cross-linked using DSP was then exposed to the cells. Exposure was allowed to proceed for 1.5 h. Cellular media was then aspirated off and a fluorescent substrate for β-Galactosidase was loaded into the cells using the influx pinocytic loading agent from Molecular Probes (Eugene, OR). The concentration of FDG exposed to cells was 1 mg/ml. Following an additional 1.5 h of incubation at 37 °C, functional activity of β-Galactosidase via FDG activation was visualized under laser confocal microscopy.

2.9. Laser Confocal Microscopy

Image acquisition was carried out using a Zeiss Axioplan 2 LSM 510 META laser confocal microscope. Excitation of GFP and FITC was carried out using an Argon laser with an excitation wavelength of 488 nm. Images were processed using the AIM software package (Carl Zeiss, Inc.) A 40X axiofluor oil immersion objective lens was utilized for the visualization of infected/transfected cells. The ocular magnification was 10X leading to a total magnification of 400X. With this microscope it is possible to generate a z-stack of images. Where indicated the z-stack is a total of 20 images taken at 1 μm intervals for a total of a 20 μm depth through the cell.

3. RESULTS

3.1. Synthesis

The synthesis for the grafting of ethylene glycol bis(succinimidyl succinate) (EGS) to polyethylenimine is outlined in Figure 1. In aqueous conditions at pH 7-9 the NHS esters of EGS (1) are reactive toward the terminal primary amines of branched form PEI at molecular weight of 1.2 kD (2). Thus the introduction of two carboxylester sites into an increased molecular weight PEI is obtained (3). The EGS grafted polyethylenimine completed synthesis was named EPI.

3.2. Characterization of PEgT

FTIR analysis was performed on the synthesized PEI analog, EPI. Figure 2 shows the IR spectrum obtained

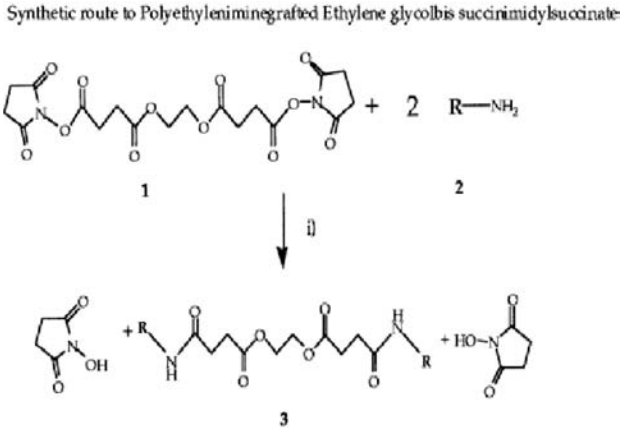

Fig. 1. Synthetic pathway for the generation of ethylene glycol bis(succinimidyl succinate) (EGS) grafted polyethylenimine (EPI). In a direct grafting reaction, NHS ester moieties on EGS (1) attack primary amines on branched form PEI of molecular weight 1.2 kD, (2) this reaction forms EGS grafted PEI (EPI) (3), and releases 2 NHS ester moieties.

for EPI. Determination of atomic bonds was done via alignment against standard correlation tables. A peak at 1100 cm^{-1} indicates the addition of an ester bond. Peak 2 at 1400 cm^{-1} is significant in that it relates to the release of the NHS ester moiety from the grafting molecule. Peak 3 located around 1650–1700 cm^{-1} indicate both the presence of a carboxyl bond and unreacted primary amines. As expected from the synthesis there is a broad stretch between 3000–3500 cm^{-1}, this is due to the large extent of amines in the initial starting material of PEI.

3.3. Size Exclusion Chromatography (HPLC-SEC)

As a first approximation for the molecular weight of the synthesized product HPLC-SEC was performed. A calibration curve was established using a range of manufacturer's published molecular weight PEI samples. The hope was that a single narrowly dispersed peak would be found. Figure 3 illustrates the refractive index detection for EPI. Again it can be seen that a single peak of relatively low dispersity is visible at 9.39 ml $\pm$ 0.02 ml. This corresponds to an approximate molecular weight of 10 kD. The second peak that is apparent on the chromatogram at 15.80 ml, is most likely due to the presence of the NHS ester reaction byproduct during the grafting process. The superimposed UV detection signal for EPI is shown in the right panel again at 254 nm. In this case the polymer again shows a single peak and there is a noted absence of the second peak present in the RI detection signal, lending confirmation to the second peak seen with RI detection as reaction byproducts. Many polymers show UV absorbance at this wavelength and the profile shows a single narrowly dispersed peak, identical in nature to that of RI detection.

3.4. Carbon-13 NMR and Dynamic Laser Light Scattering

Carbon-13 NMR was performed as a more definitive assay for the successful synthesis of the grafted product. To serve as a reference point, the starting material of PEI having a molecular weight of 1.2 kD was analyzed. The resultant spectrum displays 8 distinct peaks as indicated in Figure 4. Table I indicates the ppm shift and the corresponding structural component of PEI for the given chemical shift.

C-13 NMR analysis for the grafting of EGS to PEI of starting molecular weight 1.2 kD was also performed. The spectrum obtained from C-13 NMR spectroscopy for EPI is shown in Figure 5. The symmetry associated with the EGS grafting agent reduces the number of peaks added to the spectrum to four. Peak A ($\delta = 38.709$) are the carbon centers associated with the carboxylic esters. Peak B ($\delta = 47.300$) and peak C ($\delta = 45.472$) are the alpha and beta carbon atoms from the carboxylic ester bonds. Peak D

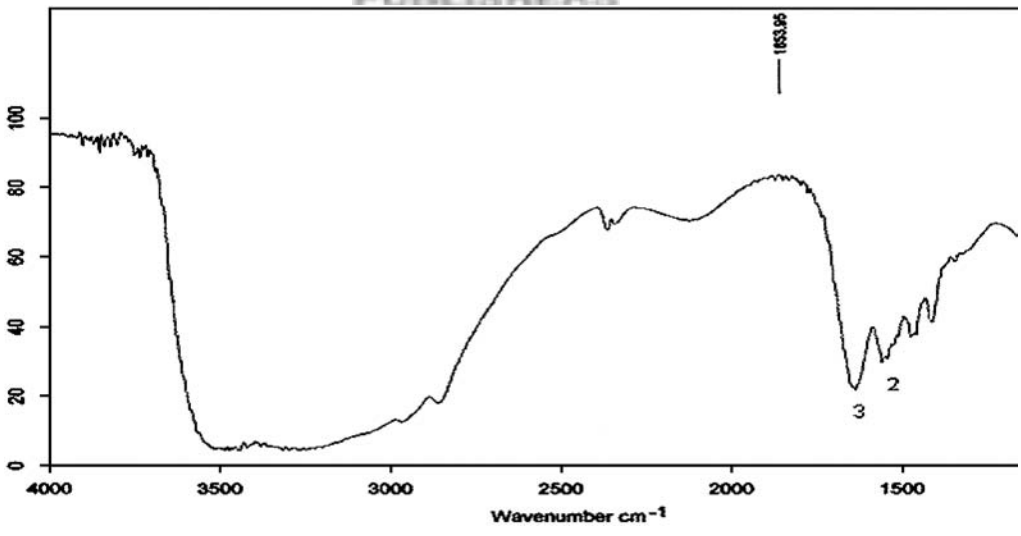

Fig. 2. FTIR spectrum for EPI. The released reaction byproducts of the NHS esters are seen in peak 2 at 1400 cm^{-1}. Peak 3 at approximately 1650–1700 cm^{-1} corresponds to the presence of the introduced carboxylester bonds.

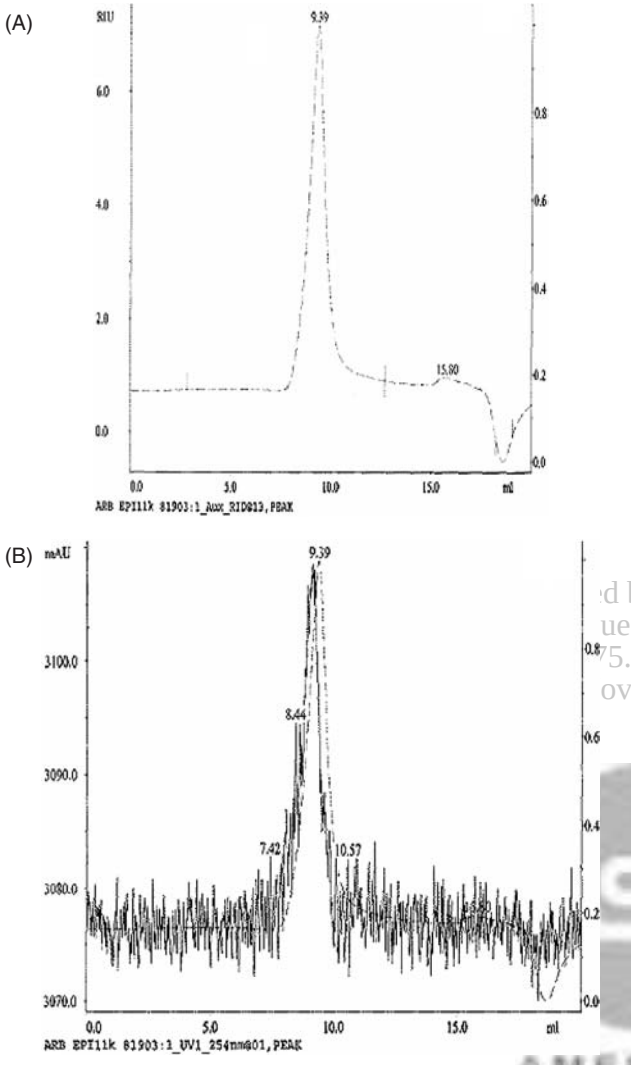

Fig. 3. Panel A: HPLC-SEC chromatogram for (EPI). Two peaks are visible, one at 9.39 ml indicative of EPI, the second at 15.80 ml indicates the release of the NHS ester molecules. Panel B: HPLC-SEC analysis of EPI using UV and RI detection. This chromatogram superimposes the UV detector response at 254 nm as a second level of confirmation of the reaction, in relation to RI detection. The column used was a Jordi Polar Pac Wax, flowing 95/5 ddH2O:acetic acid at 1.0 ml/min.

($\delta = 181.462$) as with earlier spectra is indicative of the formation of the iminoester bond between 1.2 kD PEI and EGS. The presence of this signal indicates that there has been a successful grafting of the EGS linking agent onto the native structure of PEI. The reaction byproducts of the released NHS esters are also visible on the spectrum, further confirming a successful reaction pathway. Peaks E ($\delta = 23.574$) and F ($\delta = 23.607$) correspond to the two carbon centers present in the symmetric NHS product. Chemical shifts and the associated structural features are listed in Table II.

In an effort to firmly establish a more accurate estimate of the molecular weight of the grafted product EPI, static laser light scattering experiments were undertaken. Determination of the dn/dc value (the change in refractive index

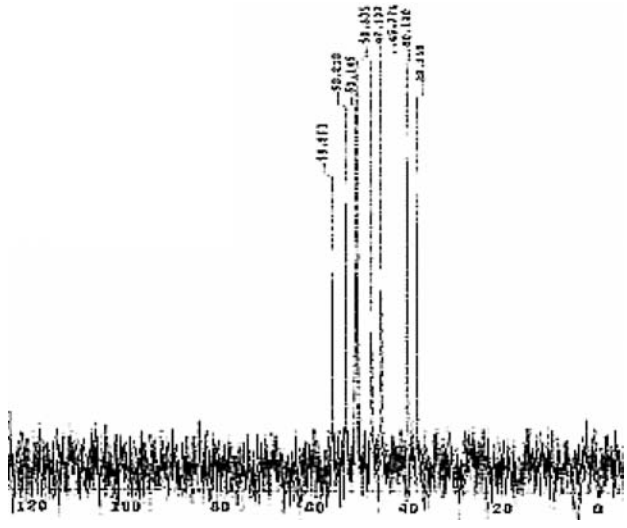

Fig. 4. C-13 NMR of native PEI at molecular weight 1.2 kD. The spectrum shows 8 distinct carbon peaks. These peaks are summarized in Table I with the corresponding structural information.

with respect to concentration) for the particular polymer was performed prior to light scattering analysis. In the case of EPI the molecular weight was estimated at 3 kD. This result was obtained under dynamic light scattering conditions (data not shown). A second set of static light scattering experiments was performed to confirm the initial results. In this series of experiments the molecular weight of EPI was seen to increase to a total mass of approximately 5 kD as the concentration of EPI was reduced in solution. Here it is seen that the estimated molecular weight of EPI is approximately 2 kD. This value is in

Table I. Chemical shift and carbon center structural identification using C-13 NMR for native PEI at molecular weight 1.2 kD.

Peak #	Chemical shift (PPM)	Structure
1	38.058	$H_2N-1-\overset{H_2}{C}-N$
2	40.190	$H_2N-2-\overset{H_2}{C}-N-$
3	45.771	$-HN-3-\overset{H_2}{C}-N$
4	47.907	$-HN-4-4-\overset{H}{N}-$
5	50.835	$-HN-5-\overset{H_2}{C}-NH_2$
6	51.146	$N-6-6-N$
7	53.213	$\overset{H_2H}{N}-7-C-N-$
8	56.263	$\overset{H_2}{N}-8-C-NH_2$

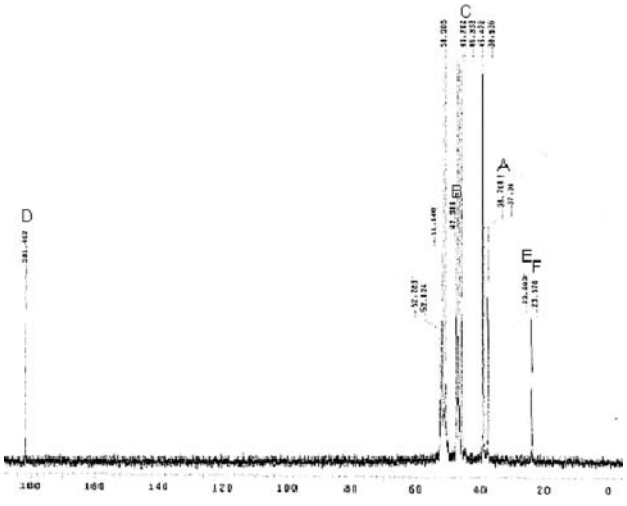

Fig. 5. C-13 NMR spectrum for (EPI). The inclusion of four peaks is consistent with the grafting of a symmetric cross-linking reagent to PEI. It is also possible to see the carbon atoms present in the reaction byproducts of the NHS ester, peaks E and F. These peaks are identified and summarized in Table II along with the corresponding structural center.

agreement with that obtained in the first set of dynamic light scattering experiments. The second virial coefficient in the case of EPI is determined to be (3.203 ± 0.577)e-3. The results for the static batch mode laser light scattering experiments are shown through the generation of a Zimm plot in Figure 6.

Table II. Peak identification and chemical shifts associated with the corresponding structural carbon centers due to the grafting of EGS to branched form 1.2 kD PEI during the generation of the synthetic product EPI.

Peak #	Chemical shift (PPM)	Structure
A	38.709	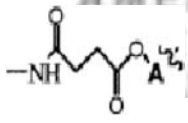
B	47.3	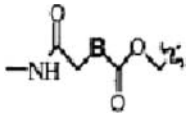
C	45.472	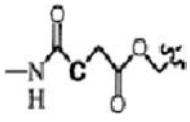
D	181.462	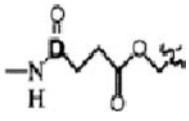
E/F	23.574/23.603	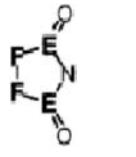

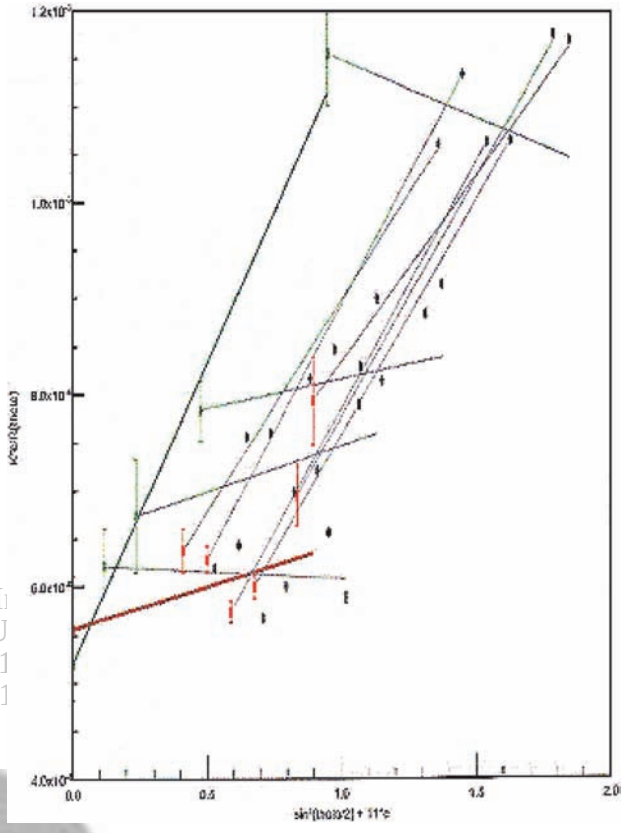

Fig. 6. Zimm plot data from light scattering experiments with EPI. Five concentrations were used in the determination of the second virial coefficient and the estimated molecular weight. The concentrations analyzed were, 5.35 mg/ml, 2.675 mg/ml, 1.34 mg/ml, 0.664 mg/ml, and 0.334 mg/ml. All samples were filtered using a 0.1 mm syringe filter.

3.5. DNA Capture and pH Buffering Capacity of EPI

To determine if alteration of the native structure of PEI during the creation of EPI ablated the intrinsic DNA condensation and capture properties of EPI, electrophoretic mobility shift assays (EMSA), and titration assays were performed. Figure 7 shows the capture of increasing amounts of plasmid DNA under a constant EPI concentration of 500 ng. Lane 1 is a standard 1 kb DNA ladder. Lane 2 represents the native plasmid DNA in linear, open circular and supercoiled forms. A similar trend in evident

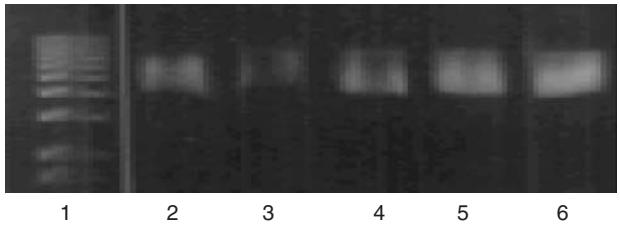

Fig. 7. EMSA for EPI. Lane 1 is 1 kb DNA ladder. Lane 2 is plasmid DNA without any capturing agent. Lanes 3–6 are 500 ng of EPI capturing increasing amounts of DNA (N/P ratios 0.75, 0.56, 0.44, and 0.36, respectively). It is evident that that EPI can successfully and spontaneously condense and capture plasmid DNA.

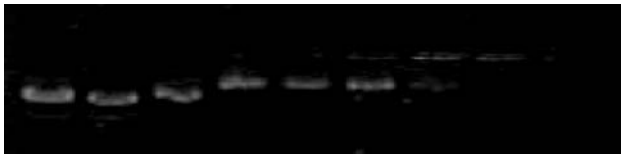

Fig. 8. EMSA for PEI capture of plasmid DNA. Lanes 1–9 show the effect of increasing an increasing amount of PEI in the presence of 1 mg of plasmid DNA. The N/P ratios used are 0, 0.15, 0.38, 0.76, 1.1, 1.5, 2.26, 3.02, 4.54, respectively. It can be seen in lane 2 that a supercoiling of the DNA has taken place due to enhanced migration toward the anode. As more PEI is present the migration begins to shift toward the cathode, lanes 4–6. In lane 7 DNA is only visible at the well indicative of a full neutralization of the charged complex. No plasmid DNA is visible in lanes 8 or 9 due to the exclusion of ethidium bromide upon PEI binding and migration toward the cathode.

in lanes 3–6 for DNA condensation and capture for EPI. Complete capture of 4 μg of plasmid DNA can be seen in lane 3. It can also be noted that in lane 6 there is diminished condensation capability of plasmid DNA with EPI due to the absence of a large supercoiled band.

Figure 8 illustrates the effects of increasing PEI concentration on electrophoretic mobility of plasmid DNA. At various N/P ratios capture of 1 μg of plasmid DNA was performed. It can be seen in lane two that there is enhanced migration of the plasmid DNA indicative of a supercoiling phenomenon occurring between the PEI and the DNA. This migration then begins to retard as more PEI becomes bound to the DNA. In lane seven it is evident that there is only DNA present at the gel well. Thus a full neutralization of the DNA phosphates has occurred. Lanes eight and nine show no DNA present indicative of ethidium bromide exclusion and migration toward the anode.

Figure 9 illustrates the results of a pH titration experiment upon EPI in comparison to the buffering capacity of native PEI at molecular weights of 1.2 kD and 10 kD. It is apparent from the figure that the synthetic product, EPI mimics the buffering capacity of 10 kD PEI.

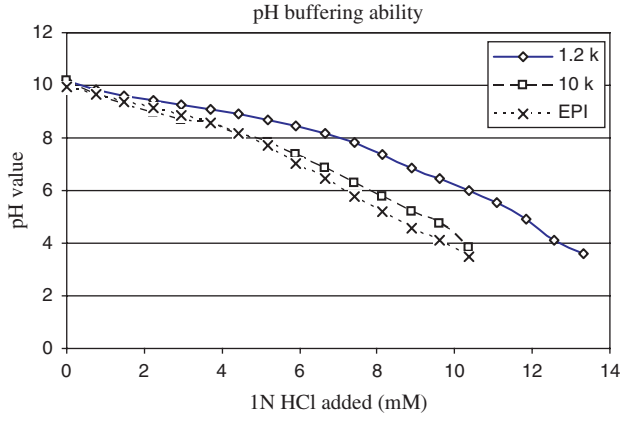

Fig. 9. pH buffering ability of EPI. pH buffering capacity of the grafted PEI analog EPI in relation to native PEI of molecular weight 1.2 kD and 10 kD. It can be seen that EPI buffers pH in a very similar fashion to that of 10 kD PEI.

3.6. GFP Plasmid DNA Transfection Through Spontaneous Capture by PEgT

In an effort to determine the ability of cells to be transfected with the grafted PEI molecule, EPI, a fluorescent assay was undertaken. To ensure that only transfection with EPI containing intact plasmid DNA occurred, a bacterial promoter system was employed. This system prevents transcription of the T7-GFP encoding plasmid DNA by mammalian transcription factors. To this end 3T3 cells were first infected with vaccinia virus Vv-T7, such that T7 RNA dependent DNA polymerase would be produced within the cytosol of the cells. This allows for the initiation of transcription of the transfected plasmid DNA within the cytosol of the cells upon successful infection by Vv-T7, the T7 polymerase, and the grafted PEI analog containing T7-GFP encoding plasmid DNA. If either of these steps fail, there would be no way to transcribe the DNA thus there would be no GFP production. Figure 10 shows the results of the transfection of 3T3 cells with 10 kD PEI. It can be seen that there is approximately 70% transfection of the 3T3 cells. It appears that the transcription of the GFP containing plasmid DNA is occurring at the cell membrane. To test the ability of PEI to fuse with the cellular membrane and create an unregulated channel, a non-membrane permeable dye (TRITC) was added to the cells concurrent with exposure to encapsulated plasmid DNA. The red fluorescence indicates the uncontrolled migration of TRITC into the cell cytosol. Transfection of 3T3 cells

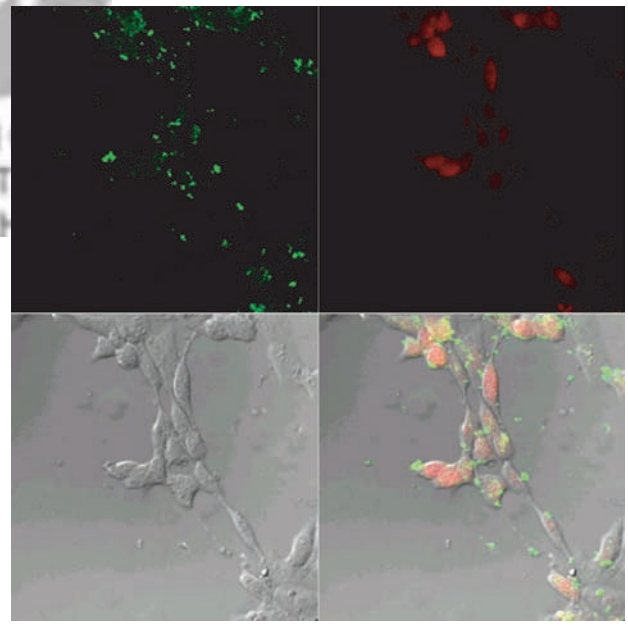

Fig. 10. Transfection of 3T3 cells with 10 kD PEI encapsulating T7-GFP encoding plasmid DNA. In this figure, cells are infected with vaccinia virus containing the bacterial T7 polymerase (Vv-T7). Subsequent transfection with PEI of 10 kD encapsulating T7 driven GFP plasmid DNA is demonstrated. Production of GFP is localized to the cellular membrane areas. TRITC is also evident within the cell cytosol and nucleus.

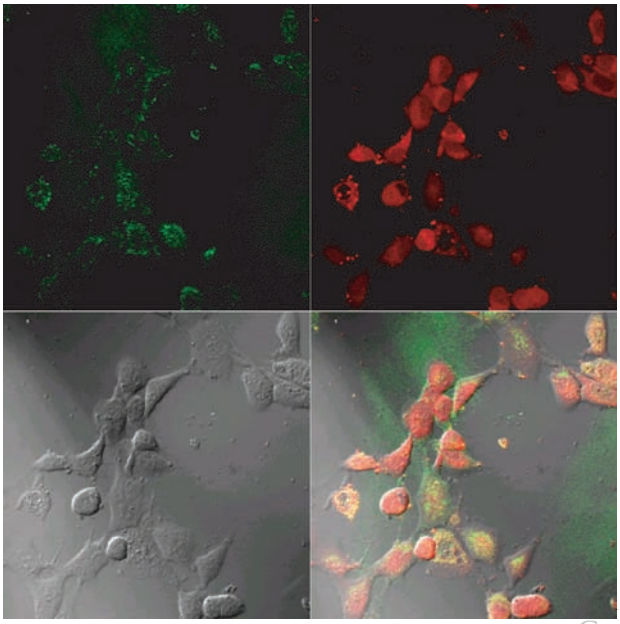

Fig. 11. Transfection of 3T3 cells with EPI encapsulating T7-GFP encoding plasmid DNA. Cells have been infected with vaccinia virus containing the bacterial T7 polymerase (Vv-T7). Subsequent transfection with EPI of 3 kD encapsulating T7 driven GFP plasmid DNA is demonstrated. GFP appears to be distributed throughout the cytosol with diminished localization to the cellular membrane areas. TRITC is also evident within the cell cytosol and nucleus.

with EPI shows both increased transfection and an increase in GFP production in Figure 11. These results demonstrate a tremendous increase in the transfection efficiency compared to other reported studies for PEI.

3.7. Transfection of 3T3 Cells with Bacterial T7 RNA Dependent DNA Polymerase

In an effort to expand to the versatility of PEI beyond that of exclusively a gene therapy vector, we investigated the ability of PEI and our grafted PEI analog EPI to transfect a large transcriptional activation protein into 3T3 cells. Such a scenario requires the delivery of a functionally active protein that is not expressed in mammalian cells. To this end, cells were first infected with vaccinia virus that contained the gene encoding beta-galactosidase (Vv-T7-Lz). This recombinant viral construct is under the transcriptional control of the T7 polymerase element. In order to visualize the production of beta-galactosidase, a synthetic marker, fluorescein di-glycosidase (FDG), was employed. FDG contains fluorescein with two tri-peptide recognition sequences for β-galactosidase attached leading to inactivation of the fluorescent properties of fluorescein. In order for FDG, to fluoresce, both substrate sites for β-galactosidase, attached to fluorescein must first be

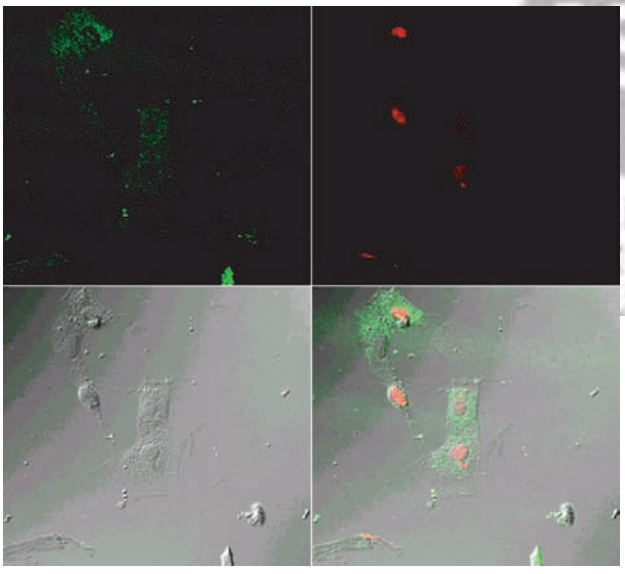

Fig. 12. Transfection of 3T3 cells with 10 kD PEI coupled to T7 polymerase via DSP. In this figure, cells have been infected with vaccinia virus containing the coding sequence for the beta-galactosidase under the control of the T7 promoter element (Vv-T7-Lz). Subsequent transfection with PEI of 10 kD coupled to T7 polymerase via DSP allows for transcription of beta-galactosidase. Visualization of active beta-galactosidase production is done using FDG loaded into the cells with the influx pinocytic cell loading reagent. GFP appears to be distributed throughout the cytosol with diminished localization to the cellular membrane areas. The presence of a cell membrane impermeable dye TRITC is also evident within the cell cytosol and nucleus. Significant cellular debris is present in the images due to osmolytic rupture upon pinocytic loading of FDG.

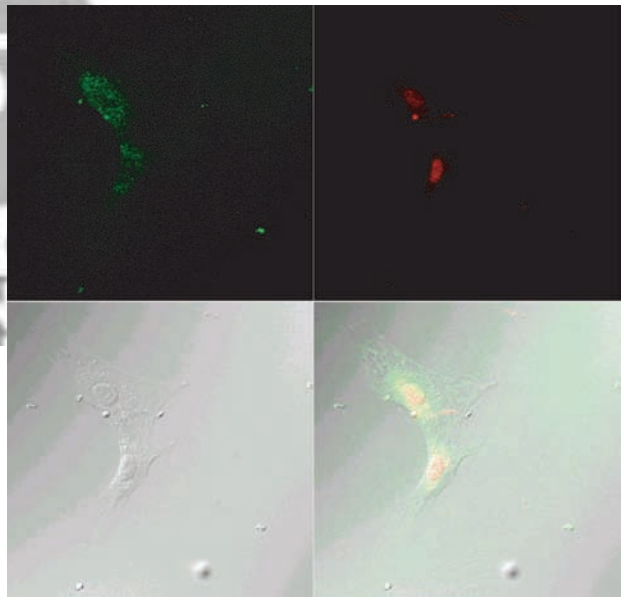

Fig. 13. Transfection of 3T3 cells with EPI coupled to T7 polymerase via DSP. In this figure, cells have been infected with vaccinia virus containing the coding sequence for the beta-galactosidase under the control of the T7 promoter element (Vv-T7-Lz). Subsequent transfection with EPI of 3 kD coupled to T7 polymerase via DSP allows for transcription of beta-galactosidase. Visualization of active beta-galactosidase production is done using FDG loaded into the cells with the influx pinocytic cell loading reagent. GFP appears to be distributed throughout the cytosol with diminished localization to the cellular membrane areas. The presence of a cell membrane impermeable dye TRITC is also evident within the cell cytosol and nucleus. Significant cellular debris is present in the images.

cleaved. Figure 12 shows the ability of PEI with molecular weight of 10 kD to transfer the T7 RNA dependent DNA polymerase into 3T3 cells. TRITC can also be visualized within the cell cytosol. There is cellular debris present in the images. The presence of the cellular debris is due to osmolytic rupture upon pinocytic loading of FDG. The efficacy of the synthesized grafted PEI analog EPI was also investigated with regard to transfection of the T7 polymerase into 3T3 cells. Figure 13 demonstrates the delivery of functionally active T7 DNA polymerase with successful release, and subsequent activation of the RNA transcript for β-galactosidase utilizing the grafted analog EPI.

4. DISCUSSION

In an effort to increase the transfection abilities of native PEI a distinct grafted copolymer was synthesized. The EGS grafted random block PEI copolymer, results in the formation of a polymer consisting of 1.2 kD PEI "monomers" that are linked together with a short linker, EGS. EGS is lyzosomally cleavable because of the introduction of two carboxylester bonds. Introduction of these specific bonding situations increases the apparent molecular weight of the polymer and should provide for the intracellular release of captured bioactive molecules. This new version of PEI was named EPI.

This cleavage releases the low molecular weight PEI monomers into the cytosol, which hopefully will reduce the cytotoxicity of the PEI based drug delivery vehicle. Examination of the FTIR spectra obtained for EPI shows the presence of an iminoester bond and the carboxylic ester bond. While it is certainly possible that this data could indicate a null reaction (i.e., unreacted EGS with the NHS esters attached to the EGS in the presence of PEI), the confirmation of a successful grafting reaction comes from the liberation of the reaction products. Importantly it can be seen that there is the presence of a signal from the NHS ester, definitively confirming the reaction success.

HPLC-SEC analysis allows an estimation of the molecular weight and polydispersity of the synthetic product. Based upon cell transfection and cytotoxicity data reported in the literature, a target molecular weight of 10 kD was determined to be optimal. Estimates of the ultimate molecular weight of the synthesized products were done through comparison against a calibration curve. In the chromatograms for EPI again a single molecular weight product of low polydispersity is formed. The elution time for EPI indicates a molecular weight of approximately 10 kD. It is important to realize that such an estimate of molecular weight is not entirely accurate for the case of EPI because the HPLC column used to construct the calibration curve is positively charged, therefore any change in the charge density of an analyte run through the column will cause an alteration in the elution time. This same inherent cationic charge on the column leads to an extended (logarithmic) elution calibration curve when PEI is analyzed. A decrease in protonatable primary amines happens to PEI upon grafting of EGS during the formation of EPI. Stochiometrically, we expect the reaction with EGS to ablate the primary amines at a minimum of two primary amines per molecule. Thus with EPI there is a loss of inherent charge possibility with an associated increase in mass. This makes estimates of molecular weight with regard to EPI suspect when using exclusion columns containing an inherent charge.

More rigorous confirmation of EPI was done using C-13 NMR and dynamic laser light scattering. To establish the baseline chemical shifts of native PEI, C-13 NMR spectroscopy was performed on PEI of molecular weight 1.2 kD. The results of this experiment correlate very well to reported values in the literature.[20,21] C-13 NMR spectroscopy of EPI indicates the presence of four new carbon atoms. The symmetry of the grafting molecule accounts for the inclusion of only four new carbon centers. The associated chemical shifts of these peaks are in agreement with published data.[20,22] Importantly it can be seen that there is an iminoester bond formed and also the liberation of the NHS ester (reaction byproduct) indicative a successful reaction.

Light scattering experiments were undertaken to obtain a more accurate estimate of the molecular weight of the grafted EPI. Investigation of EPI in two sets of experiments led to an approximation of molecular weight. Estimates of molecular weight obtained through light scattering experiments show an approximate molecular weight of 3 kD. The second virial coefficient was found to be positive indicating the presence of a very good solvent system, that being, distilled deionized water. This explains why concentration differences between the first and second set of experiments, again three fold higher in the first set, display the same molecular weight. Aggregation should be minimized due to the ability of water to solvate the EPI construct. It is also interesting that as the concentration of EPI continues to decrease, the apparent molecular weight continues to increase to approximately 5 kD. Again the ability of the EPI construct to expand in the solvent can account for such behavior. The inclusion of the two carboxylester bonds and two carbonyl functionalities could account for such a drastic change in the behavior of the synthetic product. As for HPLC-SEC analysis the ablation of the primary amines would lead to a lower charge density and therefore longer retention times on charged columns. This coupled with an exponential calibration curve could easily account for the estimated molecular weight differential between light scattering experiments and HPLC-SEC.

Plasmid DNA condensation and encapsulation properties were also investigated for EPI. If the synthetic product is incapable of entrapping DNA or protecting the DNA from intracellular environments, then they serve no utility as gene therapy vectors. Using EMSA it was seen that there is complete capture of 4 μg of DNA in the presence of 500 ng of EPI. Thus, EPI retains the ability to

spontaneously capture DNA. Upon increasing the amount of plasmid DNA present under fixed concentrations of EPI, total plasmid DNA capture is diminished then lost. The diminished ability of EPI in condensation of plasmid DNA is not unexpected due to the loss of primary amines, which are partly responsible for the capture of DNA. There is evidence, however, that there is still condensation of the DNA occurring. Titration of EPI showed a remarkably similar profile for that of 10 kD PEI. Such an observation leads to the conclusion that the grafted PEI analog is still capable of serving as a proton sponge within cells.

The ability of the derived synthetic analog of PEI to transfect cells was investigated. It was found that EPI is capable of transfecting cells to a greater extent than that of unmodified 10 kD PEI with respect to plasmid DNA. It is interesting to note that the observed transfection levels of unmodified 10 kD PEI are very high. It seems that most of the cells exposed to PEI produce GFP to some extent. This would lead to a transfection level of approximately 70 percent, a tremendous increase in the ability of native PEI when compared to published values of transcriptional activation. The transfection levels observed for EPI encapsulation of T7-GFP plasmid DNA are even greater than those seen in the case of native PEI approaching 95%.

In an effort to extend of the ability of PEI to serve as more than a gene therapy vector, coupling of protein to the cationic backbone was investigated. In this coupling reaction, an active transcription factor, T7 DNA polymerase, was linked to PEI or the grafted analogs EPI via a disulfide bond contained within the cross linking reagent DSP. This bonding situation should be easily reduced within the cytosol following successful transfection of the cell. In order for the transfection of T7 polymerase to be monitored, the cells were first infected with vaccinia virus that would produce β-galactosidase, if and only if, active T7 polymerase was delivered to the cell. A second restriction placed upon the cells is that should β-galactosidase be produced, fluorescence can only be visualized if the β-galactosidase is in an active and functional form such that cleavage of the fluorescent substrate FDG is possible. Indeed this is seen to be the case.

Transfer of the T7 polymerase to 3T3 cells can be accomplished through the linkage of T7 polymerase to the cationic backbone of PEI. The levels of fluorescence are lower than those seen for plasmid DNA delivery, a result that is not entirely unexpected. It was found that pinocytic loading of the cells with FDG frequently lead to osmotic rupture of the cellular membrane. This fact, combined with the inherent disruption of the cell cytoskeleton from vaccinia virus and cellular membrane compromise due to PEI exposure certainly accounts for a tremendous amount of the reduction in signal. This osmotic rupture also accounts for the cellular debris present in the microscopy images for protein delivery. It is interesting that with the grafted version of PEI that there is a greater degree of intracellular fluorescence. Since viral exposure concentration and time were identical, and FDG pinocytic loading conditions were identical; the only possibility that could account for such an observation is that EPI is less membrane disruptive to the cell line. This supports the concept that PEI and the synthetic derivatives thereof undergo membrane fusion rather than endocytosis.

These results suggest several alternatives to current opinions regarding delivery of substances with PEI or PEI analogs as effective delivery systems. The pathway for PEI delivery of bioactive agents into cells may occur through cellular membrane fusion. This is one possibility for the observed influx of TRITC into the cell cytosol. Endocytosis of TRITC would lead to the sequestering of TRITC into lysosomal compartments within the cell and very localized containment. Such a result is not seen as TRITC is uniformly dispersed throughout the cell cytosol, consistent with diffusional migration of a substance. The production of GFP at the cellular membrane upon transfection with 10 kD PEI bolsters this argument. Upon fusion with the cellular membrane PEI would release the encapsulated plasmid DNA to the immediate cytolsolic area of fusion. Transcription would then be initiated at that location. The apparent blebbing of GFP into the extracellular space is also suggestive of the formation of a freely permeable channel with which GFP could escape from the cells.

EPI shows diminished GFP production or localization at the cellular membrane. The incorporation of the cleavable sites within EPI could allow for a slight resealing of the cell membrane leading to a "leaky" cell. These observations also support the cytotoxicity data from earlier experiments preformed in our laboratory. The diminished cytotoxicity implies initial necrosis of the cells due to a high dose, following cleavage of the grafted PEI analog, apoptotic cell death dominates the loss in viability. Hence what was seen in the cytotoxic response was an initial insult to the cells leading to the death of a certain percentage of the cell population. This is followed by a prolonged attempt of the cells to recover from the trauma of drug exposure until apoptotic death or cellular division.

A second crucial factor to the transcriptional levels observed in our studies is the use of a transcriptional activating system that is functional within the cytosol of the cells. The first step in the transfection of 3T3 cells with plasmid DNA was the infection of 3T3 cells with vaccinia virus. This virus releases RNA into the cytosol and begins to replicate the viral genome. It is also important to note that vaccinia virus will replicate and destroy the cells within 6–8 h of infection. Upon infection with the virus and subsequent replication, the cells will begin to produce the T7 transcription factor. This transcription factor is then present in the cytosol of the cell to transcribe the delivered T7-GFP plasmid DNA. The provision of undergoing transcription within the nucleus of the cell has been removed in our particular system. The diminished transcriptional activation levels observed by many groups with regard to plasmid DNA delivery by PEI could be accounted for,

due to cytosolic DNA transcription. If this were the case, the utilization of a cytosolic trigger for the initiation of a delivered product using PEI or a PEI derivative should be significant.

Regardless, there is an enormous increase in the transfection ability and transcriptional activation of plasmid DNA. It is impossible to say if the inclusion of a disulfide bond leads to a difference in transcriptional activity. This same implication of cytosolic transcriptional activation explains why in actively dividing cells, higher transcriptional activity has been observed and also implies that there is little nuclear transport of PEI unless high does of polymer are exposed to the cells. Unfortunately, we have as of this time not tested either native PEI or the grafted analogs of PEI for transcriptional activation using a mammalian promoter system.

The product synthesized was EGS grafted to PEI (EPI). This synthetic pathway was used to introduce two carboxylester bonds that, in a majority of cell types, are cleavable within the lyzosome by carboxyl esterases. It was seen that a single molecular weight polymer with relatively low polydispersity was formed having an approximate molecular weight of 3 kD. Confirmation by both FTIR and C-13 NMR indicates a successful grafting with EGS. EMSA demonstrated that EPI is capable of DNA capture, albeit slightly diminished, and that the pH buffering capacity of EPI is similar in nature to that of 10 kD PEI. We find very high transcriptional activation of GFP encoding plasmid DNA when delivered with our synthetic product EPI. We were also able to successfully deliver a functionally active protein to fibroblasts. The culmination of these experiments represents the first known transfection of cells with an active transcriptional factor utilizing PEI or a synthetic analog of PEI as the delivery system.

References and Notes

1. W. T. Godbey and A. G. Mikos, Recent progress in gene delivery using non-viral transfer complexes. *J. Controlled Rel.* 72, 115 (**2001**).
2. W. T. Godbey, Wu, K. Kenneth, and A. G. Mikos, Poly(ethylenimine) and its role in gene delivery. *J. Controlled Rel.* 60, 149 (**1999**).
3. W. T. Godbey, M. A. Barry, P. Saggau, K. K. Wu, and A. G. Mikos, Poly(ethylenimine)-mediated transfection: A new paradigm for gene delivery. *J. Biomed Mater. Res.* 51, 321 (**2000**).
4. W. T. Godbey, K. K. Wu, and A. G. Mikos, Tracking the intracellular path of poly(ethylenimine)/DNA complexes for gene delivery. *PNAS* 96, 5177 (**1999**).
5. Y. Yamazaki, M. Nango, and M. Matsuura, Polycation liposomes, a novel nonviral gene transfer system, constructed from cetylated polyethylenimine. *Gene Therapy* 7, 1148 (**2000**).
6. O. Boussif, F. Lezoualc'h, and M. A. Zanta, A versatile vector for gene and oligonucleotide transfer into cells in culture and in vivo: Polyethylenimine. *PNAS* 92, 7297 (**1995**).
7. T. Bieber, W. Meissner, S. Kostin, A. Niemann, and H. Elsasser, Intracellular route and transcriptional competence of polyethylenimine-DNA complexes. *J. Controlled Rel.* 82, 441 (**2002**).
8. W. Guo and R. Lee, Receptor-targeted Gene delivery via Folate-conjugated polyethylenimine. *AAPS Pharmsci.* 4, 1 (**1999**).
9. C. Rudolph, U. Schillinger, and C. Plank, Nonviral gene delivery to the lung with copolymer-protected and transferring-modified polyethylenimine. *BBA* 1573, 75 (**2002**).
10. R. Kricheis, A. Kichler, and G. Wallner, Coupling of cell-binding ligands to polyethylenimine for targeted gene delivery. *Gene Therapy* 4, 409 (**1997**).
11. C. Ahn, S. Chae, Y. Bae, and S. Kim, Biodegradable poly(ethylenimine) for plasmid DNA delivery. *J. Controlled Rel.* 80, 273 (**2002**).
12. G. Tang, J. Zeng, and S. Gao, Polyethylene glycol modified polyethylenimine for improved CNS gene transfer: effects of PEGylation extent. *Biomaterials* 24, 2351 (**2003**).
13. S. Sung, S. Min, and K. Cho, Effect of polyethylene glycol on gene delivery of polyethylenimine. *Biol. Pharm. Bull.* 26, 492 (**2003**).
14. J. Benns, R. Mahato, and S. Kim, Optimization of factors influencing the transfection efficiency of folate-PEG-folate-graft-polyethylenimine. *J. Control Rel.* 79, 255 (**2002**).
15. D. Wang, A. Narang, and M. Kotb, Novel branched poly(ethylenimine)-cholesterol water-soluble lipopolymers for gene delivery. *Biomacromolecules* 3, 1197 (**2002**).
16. K. Sagara, and S. Kim, A new synthesis of galactose-poly(ethylene glycol)-polyethylenimine for gene delivery to hepatocytes. *J. Control Rel.* 79, 271 (**2002**).
17. S. G. Martin and J. C. Murray, Gene-transfer systems for human endothelial cells. *Adv. Drug Delivery Rev.* 41, 223 (**2000**).
18. L. Poulain, C. Ziller, and C. D. Muller, Ovarian carcinoma cells are effectively transfected by polyethylenimine (PEI) derivatives. *Can. Gene Ther.* 7, 644 (**2000**).
19. W. Godbey, K. Wu, and A. Mikos, Size matters: Molecular weight affects the efficiency of poly(ethylenimine) as a gene delivery vehicle. *J Control Rel.* 58, 268 (**1998**).
20. D. Axelson and S. Blake, Multinuclear (^{13}C, ^{15}N) NMR study of polyethyleneimine-based polymers. *J. Polymer Sci. Polymer Chem Ed.* 23, 2507 (**1985**).
21. St. T. Pierre, and M. Geckle, ^{13}C-NMR analysis of branched polyethylenimine. *J. Macromol. Sci-Chem.* A22, 877 (**1985**).
22. K. Pihlaja, Carbon-13 NMR chemical shifts in structural and stereochemical analysis. VCH, New York (**1994**), p. 379.

Received: 2 August 2006. Revised/Accepted: 4 December 2006.